Physics of the Earth and Planetary Interiors 282 (2018) 49–59

Contents lists available at ScienceDirect

Physics of the Earth and Planetary Interiors

journal homepage: www.elsevier.com/locate/pepi

Geomagnetic field in the Near East at the beginning of the 6th millennium BC: Evidence for alternating weak and strong intensity variations

Stanislava Yutsis-Akimova[a,b,*], Yves Gallet[a], Natalia Petrova[c], Sophie Nowak[d], Maxime Le Goff[a]

[a] Institut de Physique du Globe de Paris, Sorbonne Paris Cité, Université Paris Diderot, UMR 7154 CNRS, F-75005 Paris, France
[b] Institute of Physics of the Earth, Russian Academy of Sciences, Moscow, Russia
[c] State Historical Museum, Moscow, Russia
[d] Plateforme Rayons X, UFR de Chimie, Université Paris Diderot, F-75013 Paris, France

ARTICLE INFO

Keywords:
Archeointensity
Secular variation
Pottery
Near East
Late Neolithic
Hassuna

ABSTRACT

This study presents new archeointensity results from the multilayered settlement Yarim Tepe I located today in Northern Iraq. Archeological evidences and new radiocarbon dates indicate that this site was occupied for about four centuries, between the end of the 7th and the beginning of the 6th millennium BC, leading to a 6.5 m-thick sequence of archeological deposits. A series of 16 groups of potsherds, with a total of 76 fragments, were collected from superimposed stratigraphic layers, with thicknesses of ~30 cm on average. Archeointensity measurements were carried out using the Triaxe procedure, which takes into account both anisotropy and cooling rate effects on thermoremanent magnetization acquisition. In this study, 114 specimens from 40 fragments have fulfilled our selection criteria and mean archeointensity results were derived from nine different groups of fragments, with a minimum of three fragments per group. According to an age model constructed using a bootstrap approach, the new archeomagnetic record spans a time interval of ~220 years between ~6070 BCE and ~5850 BCE. No significant intensity variations were observed during this time interval, with an overall mean intensity value of 42.0 ± 1.6 μT. A comparison of the Yarim Tepe I data with other archeointensity results spanning the 7th and 6th millennia BC previously obtained from the Near East, as well as from Eastern and Western Europe was conducted. The Yarim Tepe I results enabled to constrain the short duration, one century at most, of an intensity peak evidenced around 5750 BCE from the Bulgarian database. Intensity variation rates associated with the ascending branch of the peak reached values as high as ~0.12–0.15 μT/year. Summarizing the geomagnetic field intensity variations in the Near East and Eastern Europe during the entire 6th millennium BC, it appears that they were likely characterized by the occurrence of two short-lasting intensity peaks at ~5750 BCE and ~5500 BCE, with intensity variation rates similar or slightly higher than the maximum rates prevailing in the modern field. Finally, it is worth mentioning that the four radiocarbon dates reported in our study provide new constraints for deciphering the temporal correlation between the cultural/historical phases (Halaf and Hassuna) that were independently defined from excavations carried out in Iraq and Syria.

1. Introduction

The accuracy of the geomagnetic field models constructed for the past millennia depends on the reliability and quantity of available data, as well as on the spatial and temporal distributions of the data. As models go further back in time, especially beyond the first millennium BC, their reliability when relying only on volcanic and archeological data is reduced. The resulting uncertainties concern all components of the geomagnetic field, including the temporal evolution of its dipole moment. Our recent studies aimed to constrain the geomagnetic field intensity behavior in the Near East during the 7th and 6th millennium BC (Gallet et al., 2015; Yutsis-Akimova et al., 2018), i.e. the two millennia following the sustained adoption of pottery in this region around 7000 BCE (e.g. Nishiaki and Le Mière, 2005; Nieuwenhuyse et al., 2010, 2013). The use of pottery during this time interval, referred to as the "Pottery Neolithic", rapidly spread to the Near East and the evolution in pottery typology and in ceramic assemblage provided essential elements for establishing local archeological chronologies in the form of a succession of cultural phases (e.g. Nieuwenhuyse et al., 2013 and reference therein).

The results dated to the 7th and 6th millennium BC currently available in the literature, in particular compiled in the global

* Corresponding author.
E-mail address: akimova@ipgp.fr (S. Yutsis-Akimova).

https://doi.org/10.1016/j.pepi.2018.07.002
Received 9 March 2018; Received in revised form 25 June 2018; Accepted 2 July 2018
Available online 04 July 2018
0031-9201/

archeomagnetic databases such as ArcheoInt (Genevey et al., 2008) and Geomagia50.v3 (Brown et al., 2015), are mostly from the Balkans, the Near East and to a lesser extent from Western Europe and from the Pacific (Hawaii). Applying a set of minimalist selection criteria (completion of an alteration test, error bars provided by the authors on their data, age uncertainties of less than ± 200 years) eliminates most of the data except those from the Balkans (Greece, Fanjat et al., 2013; Bulgaria, Kovacheva et al., 2014), and the Near East (Nachasova and Burakov, 1998; Gallet et al., 2015; Yutsis-Akimova et al., 2018), with a very few data also remaining from Western Europe (Italy; Tema et al., 2016). It thus appears that Bulgaria and the Near East, two very close areas most likely characterized by the same geomagnetic field behavior, are the only locations where a certain temporal evolution of the geomagnetic field intensity can be recovered.

The construction of a detailed intensity variation curve in the Near East for this time interval is of particular interest to deciphering the possible occurrence of extremely rapid fluctuations on a regional scale. Such features are attracting much attention in our community since the discovery of geomagnetic spikes in the Near East at the beginning of the first millennium BC (e.g. Ben-Yosef et al., 2009; Shaar et al., 2011). If confirmed, these events would be exceptional in the sense that they would be associated with intensity variation rates as high as several μT/year, much higher than the strongest rates prevailing in the modern field (~0.10 μT/year), and far beyond our present understanding of geodynamo processes (Livermore et al., 2014). The 6th millennium BC appears to be characterized by two short-lasting and intense intensity peaks observed at ~5750 BCE and ~5500 BCE (Kovacheva et al., 2014; Gallet et al., 2015; Yutsis-Akimova et al., 2018), which could eventually represent new geomagnetic spikes. The archeointensity data from the Halafian site Yarim Tepe II (Northern Iraq) recently acquired by Yutsis-Akimova et al. (2018) allowed one to further constrain the duration and the variation rates associated with the peak around 5500 BCE. If its duration seems compatible with that of geomagnetic spikes (a few decades or a century at most), the most probable variation rates estimated for this peak on the basis of a bootstrap approach (~0.15–0.25 μT/year) are significantly smaller, by one order of magnitude, than those associated with spikes. The oldest peak, which is presently only described by the Bulgarian data (Kovacheva et al., 2014), remains less well constrained and requires further investigation.

The present study is part of our effort to densify the archeointensity database in the Near East for the Pottery Neolithic period. Our main objective is to bring new constraints on the occurrence of rapid, perhaps extreme events in the intensity secular variations. This work complements a previous study conducted on a time sequential series of groups of potsherds dated to between ~5750 BCE and ~5150 BCE discovered in Yarim Tepe II (Yutsis-Akimova et al., 2018). The new archeointensity data obtained from the multi-layered site Yarim Tepe I (Northern Iraq; hereafter also referred to as YTI) dated to the Hassuna period are even older and they are amongst the oldest archeomagnetic data ever obtained. We also report on new radiocarbon dates from bone fragments found at Yarim Tepe I. The latter allow the construction of an age model for the YTI sequence and they also help to evaluate the correlation (or synchronization) between different cultural phases that, because of historical and political reasons, were independently identified in several regions of Upper Mesopotamia (in particular in Syria and Iraq).

2. Archeological setting, archeomagnetic sampling and dating

Yarim Tepe I ($\lambda = 36^{o}20'25''$ N, $\varphi = 42^{o}21'8''$ E) is a Late Neolithic multilayered settlement in the Sinjar valley, nowadays situated in Northern Iraq, about 50 km west of the city of Mosul (Fig. 1). Located in the vicinity of two other archeological sites named Yarim Tepe II and III, it was thoroughly excavated by Soviet archeologists in the late 1960s-early 1970s (Munchaev and Merpert, 1981; Merpert and Munchaev, 1987).

Initially, the Yarim Tepe I site likely spread over an area of ~2 ha, but at the time of excavations, the diameter of the tell was only about 100 m. The surface of excavations reached ~1700 m^2 for the upper levels, whereas the lower levels were excavated over an area of 400 m^2 (Munchaev and Merpert, 1981; Merpert and Munchaev, 1987). The archeological sequence comprises ~6.5 m of cultural deposits, down to 1.5 m underneath the present soil level. The entire sequence was divided into 12 archeological levels (from I to XII counted from the top to the bottom of the sequence), mainly based on building horizons distinguished from the architectural features and on the evolution of pottery style. The thickness of these levels ranges from 0.3 m to 1.10 m. Detailed description of the ceramic sequence, showing varying assemblages of both relatively coarse and painted fine wares, can be found in Merpert and Munchaev (1987). There is no doubt that the ceramics are dated to the Hassuna cultural phase first evidenced in Northern Iraq at the eponym site of Tell Hassuna (30 km south of Mosul; Fig. 1), which is currently dated to be between the end of the 7th millennium BC and the beginning of the 6th millennium BC (see for instance in Bernbeck and Nieuwenhuyse, 2013). Merpert and Munchaev (1987) distinguished two periods represented in YTI: the Archaic Hassuna from level XII to level VII, the latter level being transitional, and the Standard Hassuna from level VI to level I (Table S1; see also Petrova, 2012). However, they pointed out that the pottery production found in the two lowermost levels, that was correlated to the Hassuna Ia phase, was different from that of the levels above. A similar observation was made in other archeological sites also located today in Northern Iraq, such as in Umm Dabaghiya, Tell Sotto and Kül Tepe (see for instance Bashilov et al., 1980; Bader, 1989). This led to the distinction of the Proto-Hassuna phase having preceded the Archaic Hassuna (e.g. Bader and Le Mière; 2013; Bernbeck and Nieuwenhuyse, 2013).

Hereafter we assume the chronological subdivision of the Yarim Tepe I sequence proposed by Bashilov et al. (1980) and Bader (1989): levels XII and XI dated to the Proto-Hassuna stage, Level X is transitional between Proto- and Archaic Hassuna, levels IX and VIII dated to the Archaic Hassuna, with the level VII transitional between the Archaic and Standard phases, and levels VI to I dated to the Standard Hassuna. The uppermost levels in Yarim Tepe I were severely disturbed by the emplacements of pits and graves, among which several graves of the succeeding Halafian period, likely associated with the occupation of site Yarim Tepe II dated to that period (e.g. Munchaev and Merpert, 1981; Yutsis-Akimova et al., 2018).

Most of the remains discovered in Yarim Tepe I are stored in a repository at the Archeological Institute in Moscow, where we performed our sampling. This sampling was conducted using the same strategy as in Yutsis-Akimova et al. (2018). We collected a time-sequential series of 16 groups of pottery fragments from superimposed 20 to 45 cm-thick stratigraphic layers assumed homogeneous in time (or undisturbed) by the archeologists (see discussion in Yutsis-Akimova et al., 2018). Each group contains three to nine potsherds (Fig. 2).

The absolute dating of the archeological layers sampled in the present study might clearly justify a lengthy discussion, which, however, is beyond the scope of our study. Most of the uncertainties on that dating arise from the fact that the excavations conducted in Northern Iraq, where the Hassuna phase was first defined (as also the Samarra phase), are more than 40 years old, while more recent excavations scrutinizing the same period of time were conducted in Syria over the past 20–30 years (Nieuwenhuyse et al., 2013 and references therein). As a consequence, there is a well-recognized problem of synchronization between cultural/historical sub-divisions that were called differently between Syrian and Iraqi sites, as in particular between the Proto-Hassuna or the Archaic Hassuna to the East and the Pre-Halaf more to the West or between the Standard Hassuna or the Samarra phase and the Proto-Halaf. Due to the lack of sufficient comparative chronological markers, there is at present neither a simple nor a fully convincing approach to make such a correlation that would lead to a precise dating of the YTI sequence. Here, we decided to rely on three sources of information: firstly, the archeological dating of YTI proposed by Bashilov

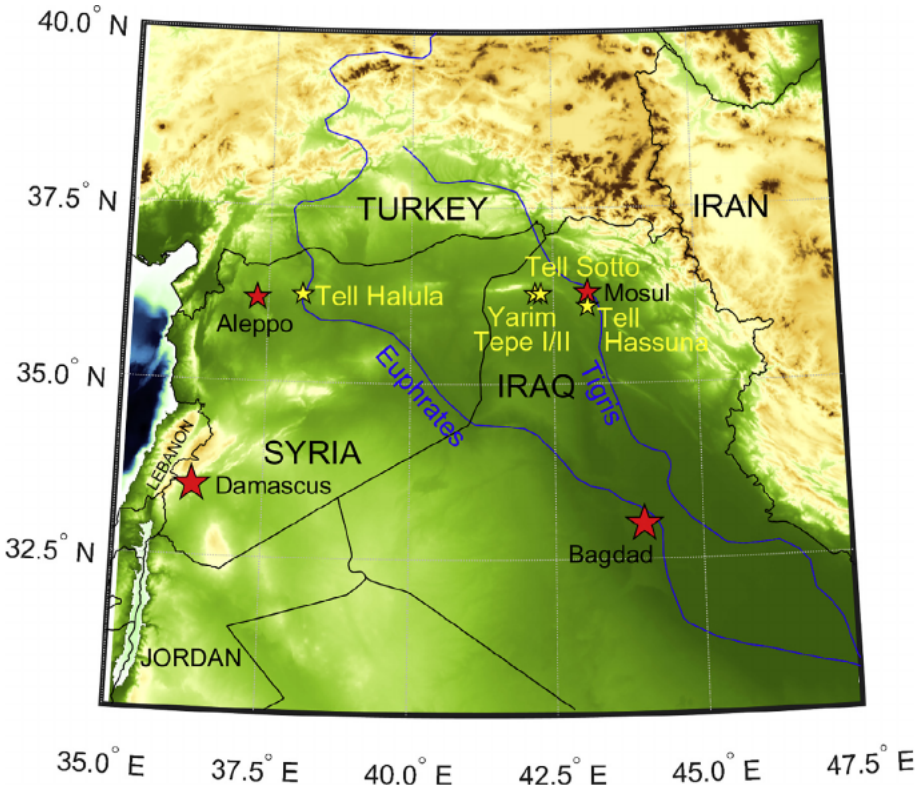

Fig. 1. Simplified general map of the Middle East showing the location of the main archeological sites mentioned in the text (yellow stars). (For interpretation of the references to color in this figure legend, the reader is referred to the web version of this article.)

et al. (1980) and Bader (1989); secondly, the standard and generally widely accepted synthesis presented by Bernbeck and Nieuwenhuyse (2013); thirdly, a set of new AMS radiocarbon dates directly obtained from the YTI sequence.

The radiocarbon analyses were carried out in the Beta Analytic dating laboratory on bone fragments recovered from four different stratigraphic layers. The radiocarbon ages were calibrated using the INTCAL13 database (Reimer et al., 2013). The results (at 95% of probability) are the following: level XI between 5.60 m and 5.80 m, 6220–6071 cal. BC (7280 ± 30 BP); level VII between 4.00 m and 4.08 m, 6016–5899 cal. BC (7080 ± 30 BP); level V between 2.85 m and 3.30 m, 5846–5720 cal. BC (6900 ± 30 BP); level V between 2.50 m and 3.10 m, 5986–5843 cal. BC (7020 ± 30 BP). It is worth mentioning that the age obtained for level VII is in agreement with two radiocarbon dates, but the latter having larger uncertainties, obtained in the 70s from the same archeological level (Campbell, 2007).

The age of the different stratigraphic layers containing the studied potsherds was derived using the same bootstrap approach as described in Yutsis-Akimova et al. (2018). The construction of the age model relied on the new ^{14}C data, together with an age arbitrarily assigned to the top of the YTI sequence. The reason for this assumption is twofold. Firstly, the two radiocarbon dates obtained for the archeological level V appear relatively scattered, which precludes the determination of a meaningful accumulation rate that could be applied up to the top of the YTI sequence. Secondly, the Standard Hassuna - Early Halaf boundary was dated at ~5900 BCE in Bernbeck and Nieuwenhuyse (2013), but

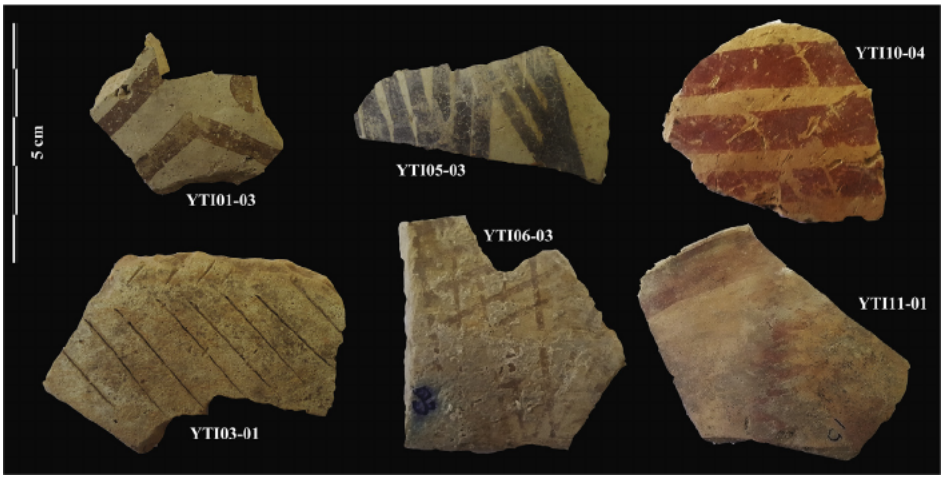

Fig. 2. Examples of potsherds from different groups collected in Yarim Tepe I. All these fragments provided archeointensity data fulfilling our Triaxe selection criteria.

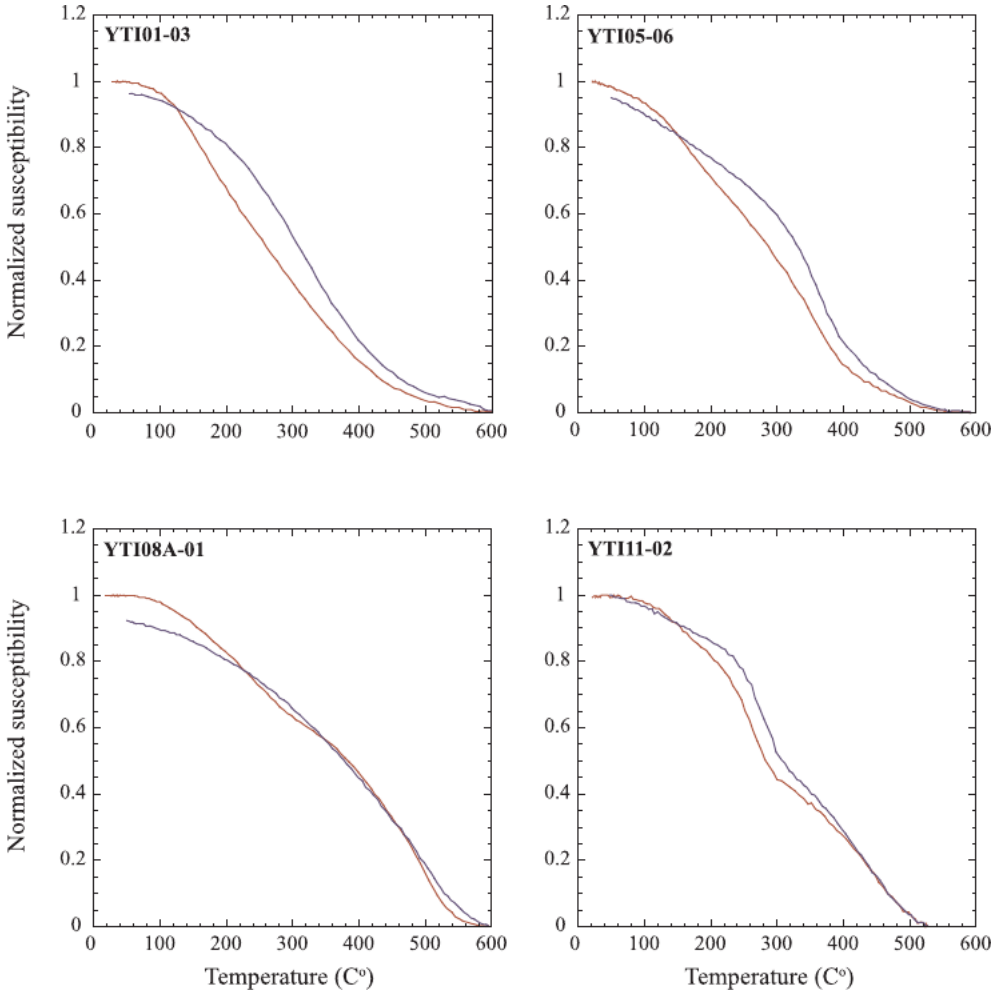

Fig. 3. Examples of low field susceptibility versus temperature curves obtained up to 600 °C from four YTI potsherds. The heating (resp. cooling) curves are in red (resp. blue). (For interpretation of the references to color in this figure legend, the reader is referred to the web version of this article.)

this age clearly appears too old when considering our new ^{14}C dates associated with the Standard Hassuna (Table S1). Those dates instead lie inside the age interval classically assumed for the Early Halaf (e.g. Molist et al., 2013; Gallet et al., 2015). This led us to assume an occupation of YTI still during the Early Halaf as defined from Syrian sites (which thus implies a temporal overlap between the Early Halaf defined in Syria and the Standard Hassuna evidenced in Northern Iraq). Two additional constraints were also retained that rely on the facts that the periods of occupation of Yarim Tepe I and Yarim Tepe II did not overlap (Merpert and Munschaev, 1987, 1993; S. Amirov pers. comm.), and that Yarim Tepe II emerged around the transition between the Early Halaf and the Middle Halaf dated at ~5750 BCE (Bernbeck and Neuwenhuyse, 2013; Molist et al., 2013; see discussion in Yutsis-Akimova et al., 2018). Taking into account all the available constraints, we considered an age of 5825 BCE for the top of the YTI sequence to which we arbitrarily attributed a reasonable uncertainty at 95% (2σ) of 75 years. On the other hand, the groups of fragments located below the stratigraphic layer having provided the oldest radiocarbon date were dated on the basis of a constant accumulation rate directly derived from the two radiocarbon dates obtained from archeological levels IX and VII.

The age model for the YTI sequence was first constructed using five tie-points. The results obtained from 10,000 bootstrap runs roughly isolate two parts, with a significant change in the accumulation rates between 3.00 and 2.00 m (red curve, Fig. S1). On average, the accumulation rates increased from ~1 cm/year in the lower part of the sequence to ~9 cm/year in its upper part. The latter accumulation rate seems very unusual and in fact rather unlikely. The high value is principally due to the ^{14}C date obtained for the stratigraphic layer between 2.85 m and 3.30 m, which appears deviant from the main temporal trend established for YTI. For this reason, we constructed an alternative age model excluding this date (green curve in Fig. S1). In this case, the accumulation rate estimated for the upper part of the YTI decreases to a much more plausible value of ~3 cm/year. Hereafter we will consider this more reasonable age model (Tables 1, S1, S2). It should be noted that the age of ~5825 BCE here considered for the top of the YTI sequence is very compatible with the age that would be determined if the very same accumulation rate deduced from the two younger remaining radiocarbon dates (i.e. obtained from the archeological level VII and from the level V between 2.50 and 3.10 m) was applied up to the top of the sequence (black dotted line in Fig. S1). Such an agreement further validates our assumption. According to our computations, it is also worth mentioning that the bottom of the YTI sequence would be dated at ~6250 BCE. Finally, our preferred age model indicates a decrease in the duration of the archeological levels between the lower and upper parts of the YTI sequence, roughly changing from ~35–40 years to ~10–15 years.

3. New archeointensity results

All archeointensity results were obtained using the experimental protocol developed for the three-axis vibrating sample magnetometer called Triaxe (Le Goff and Gallet, 2004). A detailed description of this procedure can be found in several papers, for instance in Le Goff and

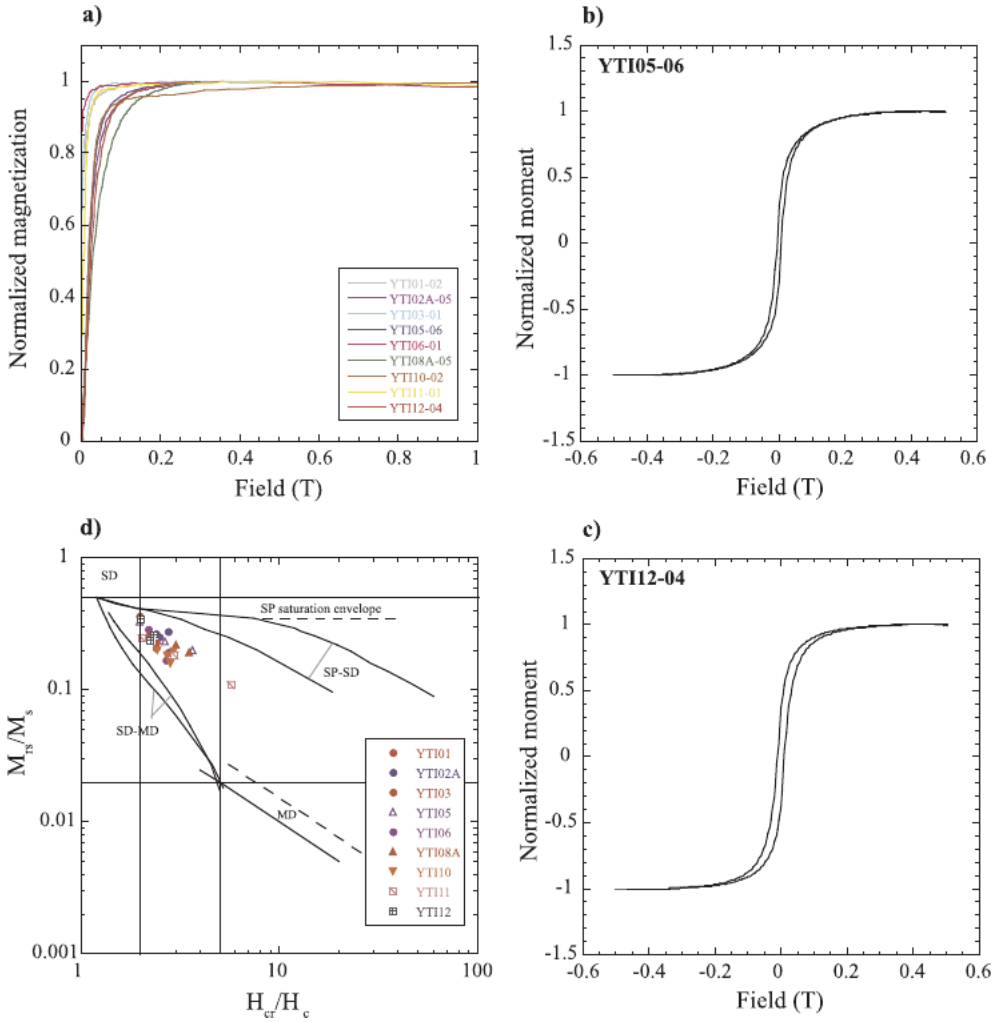

Fig. 4. Magnetic properties of YTI potsherds. (a) IRM acquisition curves obtained in fields up to 1 T. (b, c) Two examples of representative hysteresis loops. (d) Hysteresis ratios determined for all fragments that provided archeointensity data reported in a Day-Dunlop diagram (Dunlop, 2002).

Gallet (2004), Genevey et al. (2009, 2013), Hartmann et al. (2011), Gallet et al. (2014) and Yutsis-Akimova et al. (2018). Here we only briefly recall that, deriving from the classical Thellier and Thellier (1959) method, it comprises the acquisition directly at high temperatures of five successive series of magnetization measurements obtained in zero field or in field. The intensity analyses are carried out between two temperatures referred to as T1, usually fixed at 150 °C, and T2 which was chosen between 500 °C and 520 °C in the present study. Note that during the data treatment, T1 can be changed into a higher temperature (T1′) when a secondary magnetization component is still observed at T1, which allows for the determination of the archeointensity values only from the ancient univectorial thermoremanent magnetization (TRM). This was generally the case for the potsherds of Yarim Tepe I. A remarkable asset of the Triaxe protocol is that the Triaxe archeointensity values routinely take into account both the anisotropy and cooling rate effects on TRM acquisition (e.g. Genevey et al., 2009; Hartmann et al., 2010, 2011; Hervé et al., 2017).

The new archeointensity data provided in Table S2 satisfied the same set of selection criteria as the one used in previous studies also reporting Triaxe data (Genevey et al., 2009, 2013, 2016; Hartmann et al., 2010, 2011; Gallet et al., 2014, 2015; Gallet and Butterlin, 2015; Yutsis-Akimova et al., 2018). These selection criteria essentially aim to eliminate the fragments revealing an inappropriate magnetic behavior (in particular due to alteration of their magnetic mineralogy during the heating or to the presence of a strong secondary magnetization component) or the data showing a large scatter either at the fragment level or at the level of a group of fragments (see for instance Table S1 in Yutsis-Akimova et al., 2018). For each retained potsherd/fragment, a minimum of two (up to n = 5) individual specimens provided successfully analyzed results, with on average a standard deviation (n greater than 2) or a standard error (n = 2) of less than 5% of the corresponding mean intensity value. A minimum of three (N > = 3) different fragments obeying the previous criteria was required to determine a mean intensity value at the level of a group of fragments, with a standard deviation always of less than 5 μT. Moreover, as in Yutsis-Akimova et al. (2018), a 3σ rejection test was also used to detect the presence of outliers in the different groups of fragments defined with N greater than 3 (see discussion in Yutsis-Akimova et al., 2018).

Thermomagnetic low-field susceptibility curves acquired using a Kappabridge unit coupled with an oven were also used to further constrain the thermal stability of the magnetic mineralogy characterizing the retained fragments (Fig. 3). In all cases, the heating (up to ~600 °C) and cooling curves show a good reversibility, which strengthens the fact that no significant alteration of the magnetic minerals occurred for these fragments during the thermal treatment. The thermomagnetic curves show a clear inflexion between 450 °C and 580 °C, which indicates a magnetic mineralogy likely dominated by minerals from the (titano)magnetite family. This predominance was further attested by hysteresis and isothermal remanent magnetization (IRM) acquisition measurements carried out using a Vibrating Sample

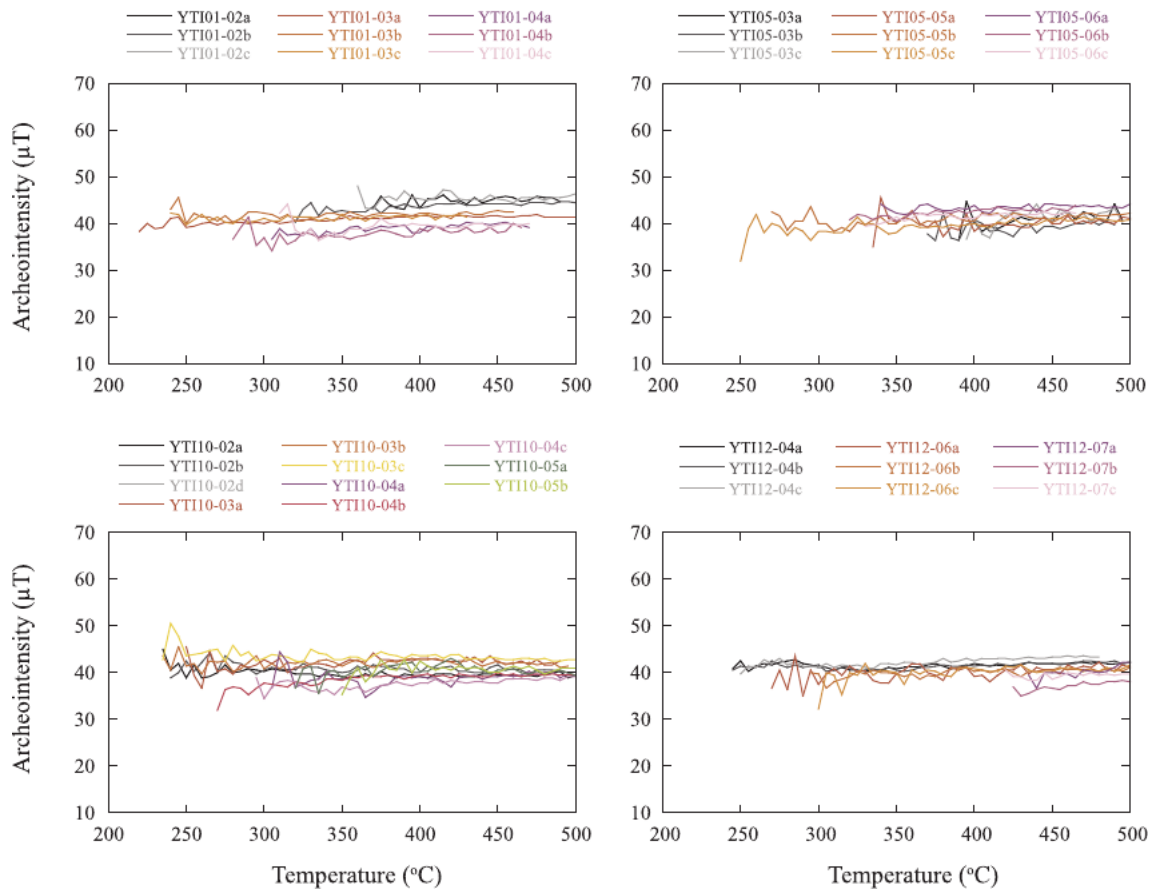

Fig. 5. Archeointensity data obtained for four groups of potsherds after the use of the 3σ rejection test. Each curve represents the R'(Ti) data obtained for one specimen over the temperature interval considered for intensity determination (see text). The data were first averaged at the specimen level, next at the fragment level and finally at the level of the group of fragments.

Magnetometer (VSM) housed in Institut de Physique du Globe de Paris (IPGP). The IRM acquisition curves obtained up to 1 T show a saturation of the magnetization achieved in fields of ~0.2–0.3 μT, with the absence of high coercivity minerals (Fig. 4a). Moreover, the hysteresis loops appear either non- or very slightly constricted (Fig. 4b,c), which also tends to eliminate the presence of a significant fraction of high coercivity minerals (such as hematite) in our collection of potsherds. When reported in a Day diagram (Dunlop, 2002), the hysteresis ratios lie inside the pseudo-single domain range of magnetite grains (Fig. 4d).

In total, we analyzed 74 fragments and 233 specimens from 16 groups of fragments. The data obtained from 40 fragments (114 specimens) fulfilled our selection criteria (Tables 1 and S2). This corresponds to a moderate success rate of ~54%, a value rather similar to that achieved for the Proto-Halafian potsherds previously analyzed from Syrian site Tell Halula (Gallet et al., 2015), with the latter pottery fragments likely being at least partly contemporaneous with those from Yarim Tepe I. We recall that the Halafian potsherds from Yarim Tepe II located in the close vicinity of YTI (Yutsis-Akimova et al., 2018) and from Tell Halula both provided a much higher success rate of nearly 70%. This difference in success rate arises at least partly from a more frequent use of the studied pottery for cooking and/or heating in the most ancient times (see below).

Most often (34 out of 40 pottery shards), the fragment-mean intensity results were determined from three individual values obtained at the specimen level (2 specimens for the six remaining fragments; Table S2). The data of four groups of fragments are reported in Fig. 5. In the different panels, each curve exhibits the R'(Ti) data obtained for one specimen over the temperature range of analysis (e.g. le Goff and Gallet, 2004). In all cases, the intensity determinations were established above 200 °C–250 °C because of the presence of a secondary magnetization component still not removed in the lower temperature range (Fig. 6). This component likely originates from a secondary firing produced for cooking purposes, even though a viscous effect is also possible. It is again worth recalling that the intensity determinations were made considering only the characteristic (primary) TRM.

Owing to our selection criteria, seven groups of fragments did not provide a mean intensity value (Tables 1, S2) because the number of retained fragments was less than 3 (two successful fragments for groups YTI-07, YTI-13 and YTI-14, only one accepted fragment for groups YTI-02, YTI-08 and YTI-09, and no fragment for group YTI-04). The two main reasons for the rejection of fragments are an inadequate paleomagnetic behavior observed during the Triaxe experiments (due to alteration) or the presence of a secondary magnetization too strong relative to the primary TRM. Moreover, among the retained groups of fragments, the use of the 3σ rejection test led to the rejection of three additional fragments (YTI02-03, YTI10-01, YTI12-01; Table S2; see also Table 1).

All group-mean intensity values are well defined with a quite small scatter. After the use of the 3σ rejection test, their standard deviations range from 0.7 μT to 3.4 μT, or from 1.7% to 8.1% of the corresponding means. We note that for the three groups revealing outliers, their standard deviation before that use still lies below the 5 μT-threshold value (Table 1). The new archeointensity results obtained in Yarim Tepe I, both at the fragment and group levels (including the three outliers), are reported in Fig. 7 according to their stratigraphic position. One can see that the intensity values remain very similar within ~5 μT at maximum and this diagram shows that no significant geomagnetic field intensity variations occurred during the occupation of this

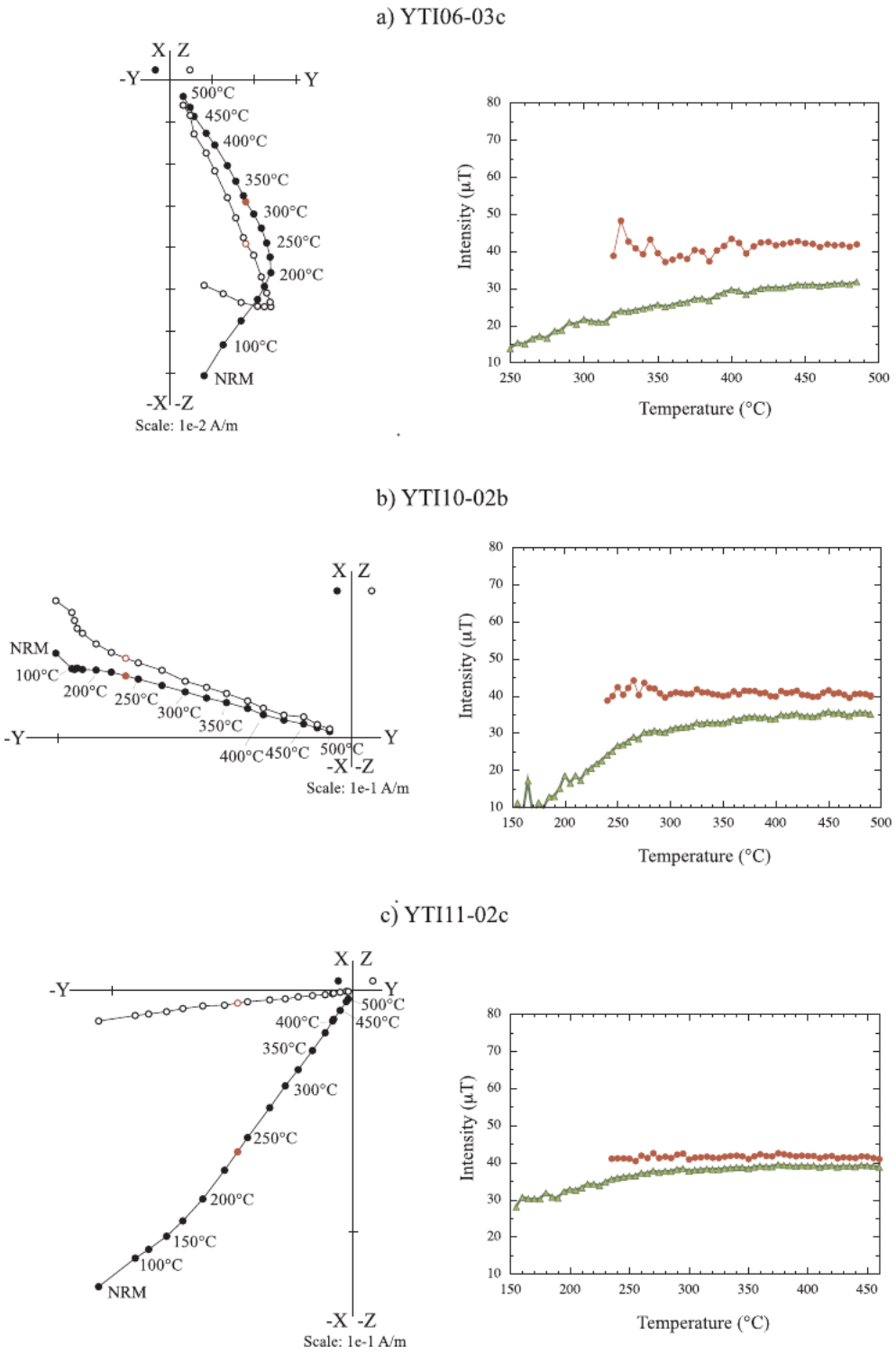

Fig. 6. Examples of thermal demagnetization diagrams obtained during the Triaxe experiments (left column). Open (close) symbols refer to the inclinations (declinations). The red point in each panel indicates the direction at temperature T1′ (see text). The corresponding R'(Ti) archeointensity data are shown in the right column between T1 and T2 (green triangles) and between T1′ and T2 (red circles). We recall that each intensity value determined at the specimen level are derived from the average of the R'(Ti) data between T1′ and T2 (Le Goff and Gallet, 2004). (For interpretation of the references to color in this figure legend, the reader is referred to the web version of this article.)

settlement. Altogether, the intensity value averaged at the level of Yarim Tepe I amounts to 42.0 ± 1.6 μT (9 groups) or 42.6 ± 2.4 μT (40 fragments).

4. Discussion

The new archeointensity results from Yarim Tepe I directly complement two other datasets previously obtained in Upper Mesopotamia, the first from Tell Sotto (Iraq; Nachasova and Burakov, 1998) and the second from Tell Halula (Syria; Gallet et al., 2015). The Tell Sotto data were obtained using the experimental procedure developed by Burakov (1981) and Burakov and Nachasova (1985), which allows correction both for TRM anisotropy and alteration effects (see also in Genevey et al., 2008). In Nachasova and Burakov (1998), however, very few details were provided on the acquisition of these results, in particular on the magnetic behavior during the thermal treatment. It is only stated that a large proportion of the samples revealed a secondary magnetization component and, as a consequence, that the intensity determinations were made on relatively high temperature ranges. Furthermore, the results were only reported in a figure, but not specified in a table.

Table 1
New archeomagnetic intensity data obtained at the fragment group level in Yarim Tepe I. The name, the stratigraphic position, the corresponding archeological level and the archeological age of the groups of potsherds are indicated in the first four columns. Their ages (± 2σ) estimated using our preferred age model are provided in the fifth column. The group-mean archeointensity results before and after the use of a 3σ rejection test and the number of fragments and specimens used for the mean computations are provided in the last three columns.

Group of fragments	Depth (m)	Archeological level	Archeological period	Age (BC) ± 2σ	Intensity (μT)	Intensity 3σ (μT)	N frag. (n spec.)
YTI-01	0.8–1.00	II	Standard Hassuna	5848 ± 52	41.6 ± 3.0	41.6 ± 3.0	3(9)
YTI-02A	0.9–1.20	III	Standard Hassuna	5854 ± 50	42.2 ± 2.6	40.9 ± 0.7	3(9)
YTI-03	1.40–1.60	IV	Standard Hassuna	5867 ± 52	44.9 ± 2.2	44.9 ± 2.2	3(9)
YTI-05	1.90–2.30	V	Standard Hassuna	5887 ± 60	41.1 ± 1.2	41.1 ± 1.2	3(9)
YTI-06	2.20–2.45	V	Standard Hassuna	5894 ± 64	42.0 ± 0.7	42.0 ± 0.7	3(9)
YTI-08A	3.30–3.60	VI	Standard Hassuna	5939 ± 58	44.1 ± 3.4	44.1 ± 3.4	3(7)
YTI-10	4.25–4.35	VII	Archaic/Standard Hassuna	5996 ± 56	41.9 ± 3.2	40.6 ± 1.7	4(11)
YTI-11	4.45–4.65	VIII	Archaic Hassuna	6024 ± 52	42.6 ± 2.2	42.6 ± 2.2	3(9)
YTI-12	4.70–5.15	IX	Archaic Hassuna	6066 ± 60	42.0 ± 3.4	40.4 ± 1.4	3(9)

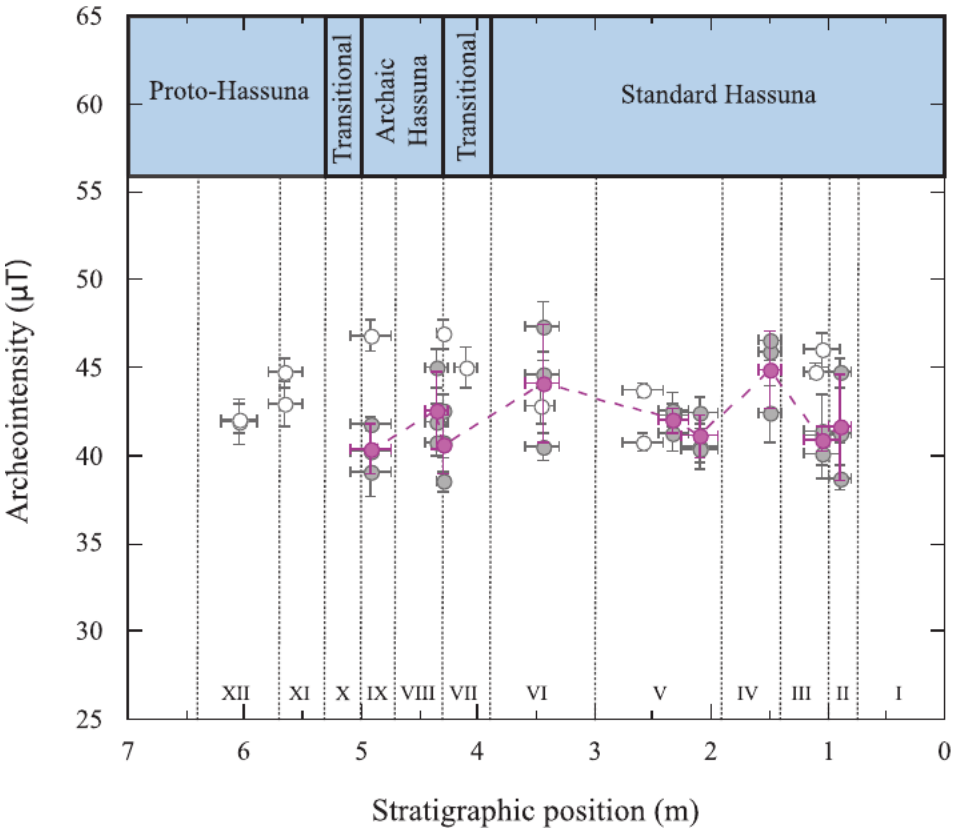

Fig. 7. New archeointensity data obtained in Yarim Tepe I as a function of their stratigraphic position. These data are both reported at the fragment level (grey dots) and, when the number of fragments fulfilling our selection criteria are is > =3, at the level of the different groups of fragments after the use the 3σ rejection test (purple dots). The open circles show the data at the fragment level for which no intensity value was determined at the group level (because of an insufficient number of fragments) or that were eliminated by the 3σ rejection test. (For interpretation of the references to color in this figure legend, the reader is referred to the web version of this article.)

Here, we use the results provided by K. Burakov to A. Genevey (A. Genevey, pers. comm.) while she was compiling the ArcheoInt database (Genevey et al., 2008). Another limitation of the Tell Sotto data is that they were misdated by Nachasova and Burakov (1998) (see also discussion in Gallet et al., 2015). Tell Sotto, which was occupied between the late Proto-Hassuna and the Standard Hassuna is largely contemporaneous with Yarim Tepe I (Table S1; e.g. Bashilov et al., 1980; Bader, 1989; Bernbeck and Nieuwenhuyse, 2013). However, according to the preliminary absolute dating in the 6th millennium BC proposed by Bader (1975; 1989) for the Tell Sotto settlement, Nachasova and Burakov (1998) assumed a time interval between ~5800 BCE and ~5500 BCE, i.e. more or less contemporaneous with that of the Middle Halaf period (Table S1; e.g. Molist et al., 2013). Such a late dating is clearly at odds with the archeological and chronological constraints currently considered. Using the dating of Yarim Tepe I (see Section 2), we thus re-dated the Tell Sotto data roughly considering that the latter site had been occupied between 6350 BCE and 5850 BCE with age uncertainties (2σ) of 75 years for these two limits (Table S1). In addition, due to the lack of information on the correspondence between the sampled stratigraphic layers and the successive archeological levels traced by the archeologists, we had to assume a constant accumulation rate throughout the entire sequence. On the other hand, the data from Tell Halula were obtained using the procedure developed for the Triaxe magnetometer and they share exactly the same set of selection criteria with the Yarim Tepe I results. Thereby, the Tell Halula and Yarim Tepe I determinations form a very homogeneous dataset. All the data discussed above are reported in Fig. 8.

Fig. 8 shows a very good agreement between the Yarim Tepe I and Tell Halula data, although the latter are few (three) for the time interval represented in YTI. In contrast, finding an agreement is more difficult with the Tell Sotto data that appear significantly higher than the new results obtained at Yarim Tepe I. Two remarks can be made. The first is that the conclusions achieved independently from the two datasets are the same, namely that no significant geomagnetic field intensity variation occurred during the occupation period of the two sites (Fig. 7 and see discussion in Nachasova and Burakov, 1998). The second point

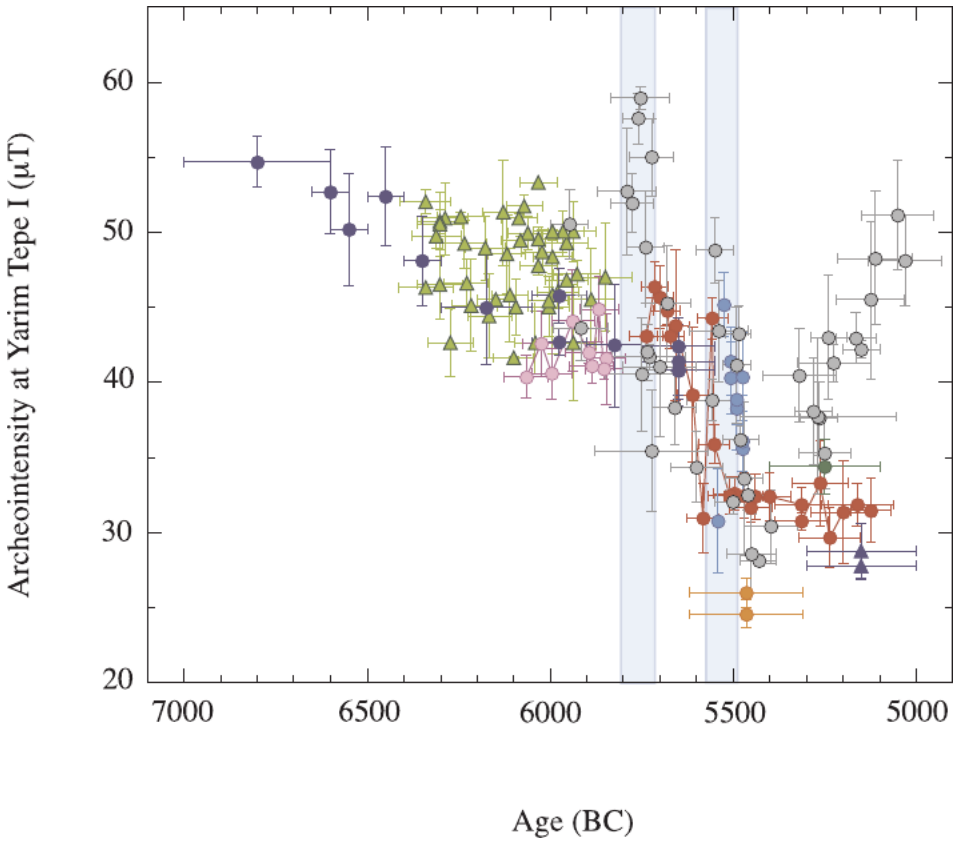

Fig. 8. Archeointensity data from the Near East and from relatively close regions (Bulgaria, Greece, Italy) presently available for the 7th and 6th millennium BC. All data were transferred to the latitude of Yarim Tepe I. The color code is the following: dark and light blue dots, Tell Halula -Syria (Gallet et al., 2015; Yutsis-Akimova et al., 2018, respectively); dark blue triangles, Tell Masaikh -Syria (Gallet et al., 2015); purple dots, Yarim Tepe I -Iraq (this study); red dots, Yarim Tepe II -Iraq (Yutsis-Akimova et al., 2018); green triangles, Tell Sotto -Iraq (Nachasova and Burakov, 1998 using a new dating discussed in the present study); grey circles, results from the Bulgarian database (Kovacheva et al., 2014); green dot, Avgi -Greece (Fanjat et al., 2013); orange dots, Portonovo -Italy (Tema et al., 2016). (For interpretation of the references to color in this figure legend, the reader is referred to the web version of this article.)

concerns the cooling rate effect on TRM acquisition, which was not taken into account in the case of the Tell Sotto data. Hence, the latter data could be reconciled with those of Yarim Tepe I by considering a cooling rate effect of ~7%, which seems to be a very reasonable and plausible estimate (Genevey et al., 2008; A. Genevey pers. comm.). Additional studies on fragments from Tell Sotto would certainly be particularly interesting, but at this stage it seems to us that the data from Tell Sotto and Yarim Tepe I are rather compatible.

Also reported in Fig. 8 are the results from the Bulgarian database compiled by Kovacheva et al. (2014) after their transfer to the latitude of Yarim Tepe I. The oldest data are slightly younger than the YTI results. However, the YTI dataset provides an interesting new constraint on the duration of the intensity peak at ~5750 BCE, i.e. around the Early Halaf - Middle Halaf transition, presently only observed from the Bulgarian data (see also the discussion in Yutsis-Akimova et al., 2018) and which might be associated with an archeomagnetic jerk (Tema and Kondopolou, 2011). When considering the data from Yarim Tepe I, it appears that the duration of this peak did not exceed a century at maximum (see the blueish zone in Fig. 8), that is a duration similar to that of the second intensity peak consistently observed at ~5500 BCE, around the transition between the Middle Halaf and the Late Halaf (Kovacheva et al., 2014, Gallet et al., 2015; Yutsis-Akimova et al., 2018). It is worth pointing out that this observation only holds if the data reported in Kovacheva et al. (2014) are reliable, what should be assessed by a complementary study focused on the Early Halaf period. A few additional archeointensity results dated to the 6th millennium BC are also shown in Fig. 8, two from Italy (Tema et al., 2016) and one from Greece (Fanjat et al., 2013). They are in good agreement with the overall trend defined by the Near-eastern and Bulgarian data.

From the archeointensity data obtained at Yarim Tepe II, Yutsis-Akimova et al. (2018) estimated the intensity variation rates associated with the peak at ~ 5500 BCE to be ~0.15–0.25 μT/year. According to the results shown in Fig. 8, it seems probable that quite similar variation rates also prevailed for the intensity peak at ~5750 BCE. To further decipher that issue, we used the same bootstrap approach as that was considered in Yutsis-Akimova et al. (2018) (see a description of the method in this article). For this, we used the intensity values obtained for YTI-01 (41.6 ± 3.0 μT) and YTI-02A (40.9 ± 0.7 μT), i.e. from the two uppermost stratigraphic layers in YTI with a group-mean archeointensity value, and successively the two Bulgarian results defining the culmination of the intensity peak around 5750 BCE (63.3 ± 0.8 μT and 62.0 ± 1.9 μT dated to 5754 ± 80 BC and 5760 ± 42 BC, respectively) after their transfer to the latitude of YTI. The most probable variation rates computed range from ~ 0.12 μT/yr to ~0.15 μT/yr (Fig. S2), and thus lie in the lower bound of the rates derived for the intensity peak at ~5500 BCE. These estimates are close to the strongest intensity variation rates prevailing in the modern geomagnetic field (e.g. Livermore et al., 2014). It is recognized that these are only rough estimates that still need to be strengthened by the acquisition of a time series of Early Halafian archeointensity results.

Finally, it is worth mentioning that the new radiocarbon dates obtained in Yarim Tepe I may indicate the need for a revision of the correlation scheme between the different phases of the Hassuna period distinguished from excavations conducted a long time ago in Iraq and the cultural/historical phases referred to as Proto-Halaf and Early Halaf that were defined more recently in Syria (e.g. Bernbeck and Nieuwenhuyse, 2013 and references therein). In contrast with what was considered so far, it appears that the Standard Hassuna characterized at Yarim Tepe I would better correspond with a time interval encompassing the recent part of the Proto-Halaf and at least the older half of the Early Halaf, between ~5980 and ~5825 BCE, rather than only with the Proto-Halaf period dated from ~6050 to ~5900 BCE (Table S1; Fig. S1). Furthermore, the Archaic Hassuna defined at Yarim Tepe I would range from the uppermost Pre-Halaf to the middle of the Proto-Halaf, between ~6090 and ~5980 BCE (Table S1; Fig. S1). This shift towards younger ages of the old Iraqi subdivisions clearly requires further investigation (and the acquisition of new radiocarbon dates), but it may offer new constraints for scrutinizing probable different time evolutions

in ceramic assemblage across the Upper Mesopotamian area.

5. Conclusions

The new archeointensity data obtained at Yarim Tepe I allow one to better constrain the geomagnetic field intensity variations in the Near East over a period of ~220 years encompassing the very end of the 7th millennium BC and the beginning of the 6th millennium BC. During this time interval, the YTI results show no significant geomagnetic field intensity variations, with a fairly stable value around 42.0 ± 1.6 μT. This relative stability would have immediately preceded a distinct intensity peak around 5750 BCE, at present only observed from archeointensity data obtained in the neighboring Bulgarian region (Kovacheva et al., 2014). Assuming that the latter results are reliable, the available dataset shows that this intensity peak lasted a century at most and that it would have involved variation rates of ~0.12–0.15 μT/year. This intensity peak would likely be of the same nature as the second peak observed soon after at ~5500 BCE (Yutsis-Akimova et al., 2018). These variation rates, even though they are very strong relative to those prevailing in the modern geomagnetic field, do not allow for the interpretation of these two peaks as being geomagnetic spikes.

The new radiocarbon dates obtained at YTI also bring new constraints on the temporal correlation between the different cultural/historical phases distinguished from the pottery data unearthed by excavations carried out in Iraq more than 40 years ago and those defined more recently in Syria. It appears that the periods referred to as Archaic Hassuna and Standard Hassuna in YTI would range from the uppermost Pre-Halaf to the younger half of the Early Halaf, with a transition around the middle of the Proto-Halaf period.

Acknowledgements

This study was partly financed by grant No. 14.Z50.31.0017 of the Russian Ministry of Science and Education. Supports by the French national program PNP/INSU-CNRS and by grant No. 16-05-00378 A of the Russian Foundation for Basic Research are also acknowledged. We are grateful to Agnès Genevey, Fernand Lopes, Olivier Nieuwenhuyse and Shahmardan Amirov for assistance and/or discussions. In particular, we thank Olivier Nieuwenhuyse for providing us important information on the Late Neolithic pottery production in Upper Mesopotamia. We also thank Evdokia Tema and an anonymous reviewer for helpful comments. This is IPGP contribution no. 3949.

Appendix A. Supplementary data

Supplementary data associated with this article can be found, in the online version, at https://doi.org/10.1016/j.pepi.2018.07.002.

References

Bader, N., 1975. Tell Sotto Early Agricultural Settlement. Sov. Archeologia 4, 99.
Bader, N., 1989. Earliest cultivators in Northern Mesopotamia. The Investigations of Soviet Archaeological Expedition in Iraq at Settlements Tell Magzaliya, Tell Sotto, and Kül Tepe. Nauka, Moscow.
Bader, N., Le Mière, M, 2013. From pre-Pottery Neolithic to Pottery Neolithic in the Sinjar. In: Interpreting the Late Neolithic of Upper Mesopotamia. Publications on Archaeology of the Leiden Museum of Archaeology (PALMA), Brepols pub. (Turnhout, Belgium), pp. 513–520.
Bashilov, V.A., Bolshakov, O.G., Kouza, A.V., 1980. The earliest strata of Yarim Tepe I. Sumer 36, 43–64.
Ben-Yosef, E., Tauxe, L., Levy, T.E., Shaar, R., Ron, H., Najjar, M., 2009. Geomagnetic intensity spike recorded in high resolution slag deposit in southern Jordan. Earth Planet. Sci. Lett. 287, 529–539.
Bernbeck, J., Nieuwenhuyse, O.P., 2013. Established paradigms, current disputes and emerging themes: the state of research on the Late Neolithic in Upper Mesopotamia. In: Interpreting the Late Neolithic of Upper Mesopotamia. Publications on Archaeology of the Leiden Museum of Archaeology (PALMA), Brepols pub. (Turnhout, Belgium), pp. 17–37.
Brown, M.C., Donadini, F., Korte, M., Nilsson, A., Korhonen, K., Lodge, A., Lengyel, S.N., Constable, C.G., 2015. GEOMAGIA50.v3: 1. general structure and modifications to the archeological and volcanic database. Earth Planets Space 67, 83.
Burakov, K.S., 1981. Determination of the ancient geomagnetic field in magnetically anisotropic specimens (Engl. Trans.). Phys. Solid Earth 17, 891–895.
Burakov, K.S., Nachasova, I.E., 1985. Correcting for chemical change during heating in archaeomagnetic determinations of the ancient geomagnetic field intensity (English Trans.). Phys. Solid Earth 21, 801–803.
Campbell, S., 2007. Rethinking Halaf chronology. Paleorient 33, 103–136.
Dunlop, D.J., 2002. Theory and application of the day plot (Mrs/Ms versus Hcr/Hc) 1. Theoretical curves and tests using titanomagnetite data. J. Geophys. Res. 107, 2056.
Fanjat, G., Aidona, E., Kondopoulou, D., Camps, P., Rathossic, C., Poidras, T., 2013. Archeointensities in Greece during the Neolithic period: New insights into material selection and secular variation curve. Phys. Earth Planet. Inter. 215, 29–42.
Gallet, Y., D'Andrea, M., Genevey, A., Pinnock, F., Le Goff, M., Matthiae, P., 2014. Archaeomagnetism at Ebla (Tell Mardikh, Syria). New data on geomagnetic field intensity variations in the Near East during the Bronze Age. J. Archaeol. Sci. 42, 295–304.
Gallet, Y., Molist, M., Genevey, A., Clop Garcia, X., Thébault, E. Gómez, Bach, A., Le Goff, M., Robert, B., Nachasova, I., 2015. New Late Neolithic (c. 7000–5000 BC) archeointensity data from Syria. Reconstructing 9000 years of archeomagnetic field intensity variations in the Middle East. Phys. Earth Planet. Inter. 238, 89–103.
Gallet, Y., Butterlin, P., 2015. Archaeological and geomagnetic implications of new archaeomagnetic intensity data from the Early Bronze high terrace "Massif Rouge" at Mari (Tell Hariri, Syria). Archaeometry 57 (Suppl. 1), 263–276.
Genevey, A., Gallet, Y., Constable, C., Korte, M., Hulot, G., 2008. ArcheoInt: an upgraded compilation of geomagnetic field intensity data for the past ten millennia and its application to the recovery of the past dipole moment. Geochem. Geophys. Geosys. 9 (4), Q04038.
Genevey, A., Gallet, Y., Rosen, J., Le Goff, M., 2009. Evidence for rapid geomagnetic field intensity variations in Western Europe over the past 800 years from new archeointensity French data. Earth Planet. Sci. Lett. 284, 132–143.
Genevey, A., Gallet, Y., Thébault, E., Jesset, S., Le Goff, M., 2013. Geomagnetic field intensity variations in Western Europe over the past 1100 years. Geochem. Geophys. Geosyst. 14 (8), 2858–2872.
Genevey, A., Gallet, Y., Jesset, S., Thébault, E., Bouillon, J., Lefèvre, A., Le Goff, M., 2016. New archeointensity data from French Early Medieval pottery production (6th–10th century AD). Tracing 1500 years of geomagnetic field intensity variations in Western Europe. Earth Planet. Sci. Lett. 257, 205–219.
Hartmann, G., Genevey, A., Gallet, Y., Trindade, R., Etchevarne, C., Le Goff, M., Afonso, M., 2010. Archeointensity in Northeast Brazil over the past five centuries. Earth Planet. Sci. Lett. 296, 340–352.
Hartmann, G., Genevey, A., Gallet, Y., Trindade, R., Le Goff, M., Najjar, R., Etchevarne, C., Afonso, M., 2011. New historical archeointensity data from Brazil: evidence for a large regional non-dipole field contribution over the past few centuries. Earth Planet. Sci. Lett. 306, 66–76.
Hervé, G., Fassbinder, J., Gilder, S., Metzner-Nebelsick, C., Gallet, Y., Genevey, A., Schnepp, E., Geisweid, L., Pütz, A., Reub, S., Wittenborn, F., Flontas, A., Linke, R., Riedel, G., Walter, F., Westhausen, I., 2017. Fast geomagnetic field intensity variations between 1400 and 400 BCE: new archaeointensity data from Germany. Phys. Earth Planet. Inter. 270, 143–156.
Kovacheva, M., Kostadinova-Avramova, M., Jordanova, N., Lanos, P., Boyadziev, Y., 2014. Extended and revised archaeomagnetic database and secular variation curves from Bulgaria for the last eight millennia. Phys. Earth Planet. Inter. 236, 79–94.
Le Goff, M., Gallet, Y., 2004. A new three-axis vibrating sample magnetometer for continuous high-temperature magnetization measurements: applications to paleo- and archeo-intensity determinations. Earth Planet. Sci. Lett. 229, 31–43.
Livermore, P.W., Fournier, A., Gallet, Y., 2014. Core-flow constraints on extreme archeomagnetic intensity changes. Earth Planet. Sci. Lett. 387, 145–156.
Merpert, N.J., Munchaev, R.M., 1987. The Earliest Levels at Yarim Tepe I and Yarim Tepe II in Northern Iraq. Iraq 49, 1–36.
Merpert, N.J., Munchaev, R.M., 1993. Yarim Tepe II: The Halaf levels. In: Yoffee, N., Clark, J. (Eds.), Early stages in the evolution of Mesopotamian civilizations: Soviet excavations in Northern Iraq. University of Arizona Press, Tucson, pp. 129–162.
Molist, M., Anfruns, J., Bofill, M., Borrell, F., Buxy, R., Clop, X., Cruells, W., Faura, J.M., Ferrer, A., Gómez, A., Guerrero, E., Saca, M., Tornero, C., Vicente, O., 2013. Tell Halula (Euphrates Valley, Syria): New approach to VII and VI millennia cal. B.C. in Northern Levant framework. In: Interpreting the Late Neolithic of Upper Mesopotamia. Publications on Archaeology of the Leiden Museum of Archaeology (PALMA), Brepols pub. (Turnhout, Belgium), pp. 443–455.
Munchaev, R.M., Merpert, N.J., 1981. Earliest agricultural settlements of Northern Mesopotamia. The investigation of Soviet expedition in Iraq (in Russian). Nauka, Moscow.
Nachasova, I., Burakov, K., 1998. Geomagnetic variations in the VI-V millennia B.C. Geomagn. Aeron. 38, 502–505.
Nieuwenhuyse, O., Akkermans, P., van der Plicht, J., 2010. Not so coarse, nor always plain -the earliest pottery of Syria. Antiquity 84, 71–85.
O.P. Nieuwenhuyse, R. Bernbeck, P.M.M.G. Akkermans, J. Rogasch, Interpreting the Late Neolithic of Upper Mesopotamia. Publications on Archaeology of the Leiden Museum of Archaeology (PALMA), Brepols pub 2013 (Turnhout, Belgium), p. 520.
Nishiaki, Y., Le Mière, M., 2005. The oldest pottery Neolithic of Upper Mesopotamia: New evidence from Tell Seker al-Aheimar, the Khabur, northeast Syria. Paléorient 31, 55–68.
Petrova, N., 2012. A technological study of Hassuna culture ceramics (Yarim Tepe I settlement). Documenta Praehistorica XXXIX 75–82.
Reimer, P.J., Bard, E., Bayliss, A., Warren, J.B., Blackwell, P., Ramsey, C.B., Buck, K., Cheng, H., Edwards, L., Friedrich, M., Grootes, P.M., Guilderson, T.P., Haflidason, H., Hajdas, I., Hatté, C., Heaton, T.J., Hoffmann, D.L., Hogg, A.G., Hughen, K.A., Kaiser,

K.F., Kromer, B., Manning, S.W., Niu, M., Reimer, R.W., Richards, D.A., Scott, E.M., Southon, J.R., Staff, R.A., Turney, C.S., Van der Plicht, J., 2013. IntCal13 and Marine13 Radiocarbon Age Calibration Curves 0–50,000 Years cal BP. Radiocarbon 55 (4), 1869–1887.

Shaar, R., Ben-Yosef, E., Ron, H., Tauxe, L., Agnon, A., Kessel, R., 2011. Geomagnetic field intensity: how high can it get? How fast can it change? Constraints from iron-age copper-slag. Earth Planet. Sci. Lett. 301, 297–306.

Tema, E., Kondopolou, D., 2011. Secular variation of the Earth's magnetic field in the Balkan region during the last eight millennia based on archeomagnetic data. Geophys. J. Int. 186, 603–614.

Tema, E., Ferrara, E., Camps, P., Conati Barbaro, C., Spatafora, S., Carvallo, C., Poidras, T., 2016. The Earth's magnetic field in Italy during the Neolithic period: new data from the Early Neolithic site of Portonovo (Marche, Italy). Earth Planet. Sci. Lett. 448, 49–61.

Thellier, E., Thellier, O., 1959. Sur l'intensité du champ magnétique tesrrestre dans le passé historique et géologique. Ann. Géophys. 15, 285–376.

Yutsis-Akimova, S., Gallet, Y., Amirov, S., 2018. Rapid geomagnetic field intensity variations in the Near East during the 6th millennium BC: New archeointensity data from Halafian site Yarim Tepe II (Northern Iraq). Earth Planet. Sci. Lett. 482, 201–212.